

Hydrodynamic response of rotationally supported flows in the Small Shearing Box model [★]

A. Sternberg¹, O.M. Umurhan^{1,2,3}, Y. Gil¹ and O. Regev^{1,4}

¹Department of Physics, Technion-Israel Institute of Technology, 32000 Haifa, Israel

²Department of Geophysics and Space Sciences, Tel-Aviv University, Tel-Aviv, Israel

³Department of Astronomy, City College of San Francisco, San Francisco, CA 94112, USA

⁴Department of Astronomy, Columbia University, New York, NY 10025, USA

Received — / Accepted —

Abstract. The hydrodynamic response of the inviscid small shearing box model of a midplane section of a rotationally supported astrophysical disk is considered. We consider comparatively the predictions to disturbances subject to different boundary conditions. All linear disturbances subject to shearing boundary conditions decay algebraically at long times and the quality of the decay, whether monotonic or oscillatory, depends on whether the parameter Σ , defined as a function of the disturbance's vertical and azimuthal wavelengths as well as the background linear shear, is greater or less than 1. These observations agree with recent published results. There is also short time growth of flow quantities and the degree of this growth depends directly on the streamwise streakiness of the mode. Linear disturbances subject to channel boundary conditions have normal-modes exhibiting inertial oscillations if $\Sigma > 1$ - otherwise disturbances must in general be treated as an initial value problem. An energy functional \mathcal{E} can also be formulated for the general nonlinear problem irrespective of the boundary conditions employed. It is found that the fate of disturbances is related to the conservation of this quantity which depends on the boundary conditions utilized. We relate these results and their implications to the question of nonlinear activity in such flows.

Key words. accretion, accretion disks – hydrodynamics – linear theory – nonlinear theory

“Extraordinary how mathematics helps you to know yourself.”

Samuel Beckett, *Molloy*

1. Introduction

Nontraditional routes to sustained hydrodynamic activity in rotationally supported Rayleigh-stable shear flows have been explored and debated over the last decade in the astrophysics community (Ioannaou & Kakouris, 2001, Longaretti, 2002, Chagelishvili *et al.*, 2003, Yecko, 2004, Mukhopadhyay *et al.* 2004, Afshordi *et al.* 2004, Umurhan & Regev, 2004, Sternberg, 2005, Lesur & Longaretti, 2005, Balbus & Hawley, 2006, Rincon *et al.* 2006, Ji *et al.*, 2006, Williams, 2006¹, Jiménez *et al.*, 2006) - where the interest

has been in resolving the source of the anomalous transport observed in accretion disk systems (for a review see Frank *et al.*, 2002). The possibility of something other than a supercritical linear normal-mode instability route to turbulence in such systems is inspired by the notion of non-normal growth and transition in subcritical flows - often referred to as *bypass transition*. This type of transition has been identified as being responsible for the maintenance of nonlinear activity of non-rotating shear flows which, otherwise, show no signs of linear instability, *e.g.*, model pipe-Pouissele flow (Butler & Farrell, 1992, Waleffe, 1997, and see Schmid and Henningson, 2000, and references therein).

Rotating incompressible *linear shear* flow models like the small shearing box, (*i.e.*, the system first considered in an astrophysical context by Goldreich & Lynden-Bell, 1965, and *SSB* hereafter) which are localized representations of midplane disk shear flow, mathematically resemble rotating plane-Couette flow (rpC for short). For parameters appropriate for an astrophysical disk the rpC flow is both anticyclonic and in the Rayleigh stable regime and, as such, no linear instabilities for it are known. Thus

Send offprint requests to: A. Sternberg, e-mail: phassaf@technion.technion.ac.il

[★] Research supported by the Israel Science Foundation, the Helen and Robert Asher Fund and the Technion Fund for the Promotion of Research

¹ Note that this work originally appeared in Williams (2000).

if sustained activity exists in these flows it must be subcritical in character. Because the linear operators in rpC flows are also non-normal it has been suggested that an analogous nonlinear bypass transition could maybe take place in those Rayleigh-stable anticyclonic cases (Yecko 2004, Mukhopadhyay *et al.* 2004, Afshordi *et al.* 2004).

There are mathematical similarities between the linearized system of equations describing the plane-Couette (pC) flow, in which amplification is through the lift-up effect (*e.g.*, Schmid & Henningson, 2000, Waleffe, 2003), and rpC flow on the Rayleigh line where amplification arises from the anti lift-up effect (Antkowiak & Brancher, 2006, Rincon *et al.*, 2006).²

Rincon *et al.* (2006) apply to rpC flow the techniques used by others to establish the presence of exact steady (possibly unstable) nonlinear solutions in pC flow but they report that no such solutions could be identified nor continued from the Rayleigh marginal line into the Rayleigh stable regime in wall-bounded rpC flow. To paraphrase their words, the phenomenology of subcritical transition in wall-bounded pC flow appears not to carry over to rpC flow near the Rayleigh line.

Thus despite the attractiveness of the bypass transition concept for Rayleigh-stable rpC flows, this recent work, as well as the recent experimental results of Ji *et al.* (2006) and numerical results of Lesur & Longaretti (2005) seem to suggest that hydrodynamic activity of *confined flows*, if at all present, generates sustained activity which appears to be at least two orders of magnitude too weak (turbulent $\text{Re} > 10^5$) to account for accretion disk observations. Similar trends in the level of turbulence from numerical models of SSB flows utilizing shearing boundary conditions (see below) are suggested by Hawley *et al.* (1999) and Lesur & Longaretti (2005) and most recently Jiménez *et al.* (2006).

From an academic standpoint (at the very least!) it is worthwhile to understand what are the reasons for the situation as it stands:

1. is it that turbulence does exist for anticyclonic Rayleigh stable rpC flow but is comprised of fluid structures that we have yet to identify,
2. is it that instigation of a turbulent transition in such flows is sensitive to initial perturbations as some authors suggest (*e.g.*, pipe-Pouissele flow, Faisst & Eckhardt, 2004) and its trigger still remains elusive for Rayleigh-stable anticyclonic rpC,
3. or is it that there is no possibility of turbulence for these flows because they are unequivocally stable?

With regards to the last point we again call attention to the results of Lesur & Longaretti (2005) wherein they

² The *Rayleigh line* is the relationship between the Reynolds numbers (Re) at the inner and outer radii of a Taylor-Couette experiment signifying the transition to axisymmetric linear instability. This relationship reflects the differences in the rotation rates between the inner and outer cylinders. (*e.g.*, see Drazin & Reid, 1983, for a discussion).

numerically demonstrate that there is sustained nonlinear activity in anticyclonic Rayleigh-stable rpC flows near the Rayleigh line meaning that there is a subcritical transition. Yet they showed that if one moves deeper into the Rayleigh-stable regime the effective turbulent transport becomes weaker. Will this trend in the transport properties persist as simulations become more resolved? The simulations performed by Jiménez *et al.* (2006) are beginning to achieve the resolution needed (Lesur & Longaretti, 2005) to properly address this question.

Far from offering a solution to this problem we instead share three results that may serve as clues in resolving this issue. To this end we reconsider the dynamics of inviscid anticyclonic Rayleigh stable flows in the SSB model (*i.e.*, rpC flow) subject to shearing boundary conditions (Goldreich & Lynden-Bell, 1965, Rogallo, 1981, Balbus & Hawley, 1992, and SBC hereafter) or channel boundary conditions (*e.g.*, Yecko, 2004, Lesur & Longaretti, 2005, Rincon *et al.* 2006, CBC hereafter).

To set the scene we initially note that there are qualitative differences (irrespective of the type of boundary conditions employed) in the behavior of *linearized disturbances* depending on whether or not the quantity Σ is less than or greater than 1. This parameter is defined as

$$\Sigma = 4 \frac{2(2-q) \ell_y^2}{q^2 \ell_z^2}, \quad (1)$$

where ℓ_z, ℓ_y are the disturbance length scales in the vertical (like the disk normal) and streamwise (like the disk azimuth) directions of any given modal disturbance. The global flow for which the SSB is meant to represent is characterized by a rotation rate Ω that depends on the radial coordinate R according to the relationship $\Omega \propto R^{-q}$. In the parlance of geophysical flows $q = -2/Ro$, where Ro is the Rossby Number as it would be defined by the rotation velocities (Pedlosky, 1987). Additionally and hereafter, we will consider linear shear profiles that are anti-cyclonic, *i.e.*, those in which $q > 0$. At $\text{Re} = \infty$ axisymmetric linear instability occurs for $q = 2$.

The first result is that for SBC, (i) individual wavemodes show algebraic decay of their amplitude irrespective of Σ however (ii) when $\Sigma < 1$ the decay is monotonic with time t but when $\Sigma > 1$ disturbances oscillate during their decay with a period that scales as $\ln t$. In general the response of the wavemode is oscillatory in character if $\Sigma > 1$. We also find that the transient response is greatest when the disturbances have large leading streamwise streaky structure. By this we mean to say those waves which *lead* the shear and whose *streakiness* is measured by ℓ_y/ℓ_x , where ℓ_x is the radial length scale of the initial disturbance. These results, reported originally in Sternberg (2005), confirm those reported by Balbus & Hawley (2006) wherein they also note that the individual wavemodes are exact nonlinear solutions when SBC are employed.

The second result relates to dynamics subject to CBC. For a given vertical and azimuthal wavenumber, if $\Sigma > 1$ the system supports a countably infinite number of normal modes that oscillate without growth or decay which

are inertial oscillations, otherwise if $\Sigma < 1$ the system allows for only one eigenmode meaning that in general the dynamical response is non-normal and must be treated as an initial value problem, a situation encountered in pC flow.

The third result is a general nonlinear feature pertaining to the energetics of such flows. If one defines \mathcal{E} as the total energy of the flow *in the SSB*, whose dynamical constituent includes the total kinetic energy, (*i.e.*, the energy formed by considering the total velocity - which is to say the velocity fluctuations plus background shear flow), the fate of \mathcal{E} depends upon the boundary conditions employed. \mathcal{E} is conserved for (but not limited to) (i) disturbances subject to CBC, (ii) azimuthally and vertically periodic, radially localized disturbances in radially unbounded domains. On the other hand, disturbances subject to SBC do not identically conserve \mathcal{E} and its temporal quality depends critically upon the dynamics within the domain.

This work is organized as follows: in Section 2 we introduce the SSB, formally state and describe the boundary conditions and derive the energy integral result. In Sections 3 and 4 we perform and present a linear analysis of the system's response subject to SBC and CBC. The solution methods here use a mixture of numerics, asymptotics and exact analysis'. In Section 5 we summarize the results and speculate as to their implications to the questions posed here in this Introduction.

2. Equations, Boundary Conditions and Two Integral Statements

2.1. Equations

There are a few formal derivations for the set of equations appropriate to the dynamics of a localized section of a rotationally supported disk. Most of these derivations arrive upon the governing equations given in Goldreich & Lynden-Bell (1965). With the external gravity set to zero and the density constant, these non-dimensionalized equations (Umurhan & Regev, 2004) are

$$\nabla \cdot \mathbf{u} = 0, \quad (2)$$

$$(\partial_t - q\Omega_0 x \partial_y)u + \mathbf{u} \cdot \nabla u - 2\Omega_0 v = -\partial_x P \quad (3)$$

$$(\partial_t - q\Omega_0 x \partial_y)v + \mathbf{u} \cdot \nabla u + (2 - q)\Omega_0 u = -\partial_y P, \quad (4)$$

$$(\partial_t - q\Omega_0 x \partial_y)w + \mathbf{u} \cdot \nabla w = -\partial_z P. \quad (5)$$

These equations represent the dynamics taking place in a "small-shearing box" (SSB for short) section near the midplane of a disk rotating about the central star with the local rotation vector, $\Omega_0 \hat{\mathbf{z}}$. The flow on these scales is equivalently known as incompressible rotating plane-Couette flow (*e.g.*, Nagata, 1986). In this form these equations are the inviscid limit of those considered by Longaretti (2002) and Yecko (2004).

In the language of this paper, x corresponds to the radial (shearwise) coordinate, y corresponds to the azimuthal (streamwise) coordinate and z corresponds to the

vertical (spanwise) coordinate, the last of these is the direction normal to the original disk midplane. The velocity disturbances in the radial, azimuthal and vertical directions expressed by the variables $\mathbf{u} = \{u, v, w\}$. These velocities represent deviations over the steady Keplerian flow (as manifesting itself in this rotating frame) given by $-q\Omega_0 x \hat{\mathbf{y}}$ - which is also known as Couette shear.

Ω_0 is sometimes also referred to as the Coriolis parameter, and in these nondimensionalized units Ω_0 is 1. Nevertheless we retain the symbol in order to flag the Coriolis effects in this calculation. The local shear gradient is defined to be

$$q \equiv - \left[\frac{R}{\Omega} \left(\frac{\partial \Omega}{\partial R} \right) \right]_{R_0}, \quad (6)$$

in which $\Omega(R)$ is the full disk rotation rate as a function of cylindrical radius R . The SSB equations represent the dynamics taking place in a localized neighborhood around $R = R_0$. For Keplerian disks $q = 3/2$. Instability to Taylor vortices occurs for $q > 2$. Thus, by *Rayleigh stable* we mean to say when $q < 2$.

2.2. Boundary Conditions

We first present and discuss the means by which one administers *shearing boundary conditions* (SBC) in the SSB. By this we mean to say that the flow variables \mathbf{u} , and p are (a) periodic in the azimuthal and vertical directions on scales $L_y = 1$ and $L_z = 1$ respectively and (b) are simply periodic³ (on scale $L_x = 1$) in the shearwise (radial) direction with respect to a coordinate frame that moves with the local shear (Lynden-Bell & Goldreich, 1965, Balbus & Hawley, 1996, and recently, Umurhan & Regev, 2004). In this work we refer to this coordinate frame as the *shearing coordinate* frame (SC for short). The standard coordinate frame, that is, the coordinate frame of an observer in the rotating frame, will be referred to as the *non-shearing coordinate* frame (NSC for short): this terminology is the same one used in Umurhan & Regev (2004). In this sense, the fundamental equations (2-5) have been expressed in the NSC frame.

If (X, Y, Z, T) represent the independent variables in the SC frame then we say they are related to the NSC variables by

$$X = x; \quad Y = y + q\Omega_0 x t \quad Z = z; \quad T = t. \quad (7)$$

If f is any dynamical quantity then in the SC frame the periodic boundary conditions in the shearwise, azimuthal and vertical directions respectively are

$$\begin{aligned} f(X, Y, Z) &= f(X + L_x, Y, Z), \\ f(X, Y, Z) &= f(X, Y + L_y, Z), \\ f(X, Y, Z) &= f(X, Y, Z + L_z). \end{aligned} \quad (8)$$

³ By *simply periodic* in some direction "a" with length scale " L_a ", we mean to say that a given dynamical quantity satisfies $f(a, b, c) = f(a + L_a, b, c)$.

Of course this means in general that $f(X, Y, Z) = f(X + L_x, Y + L_y, Z + L_z)$. As expressed in the NSC frame, the periodicity in the azimuthal and vertical directions appears like

$$f(x, y, z) = f(x, y + L_y, z), \quad f(x, y, z) = f(x, y, z + L_z),$$

while the periodicity in the shearwise direction appears in the NSC frame as

$$f(x, y, z) = f(x + L_x, y + q\Omega_0 t L_x, z).$$

Because of the periodicity in the azimuthal (y) direction this statement takes the form $f(x, y, z) = f(x + L_x, y + \tilde{y}, z)$ where $\tilde{y}(t) = q\Omega_0 t L_x \pmod{L_y}$. Note that this means that only after *exactly* integer values of $q\Omega_0 t L_x / L_y$, (*i.e.*, when $\tilde{y} = 0$) are the SC and NSC frames coincident. This means that this coincidence repeats every

$$T_{\text{rep}} = L_y / q\Omega_0 L_x \quad (9)$$

time units. Evidently the SBC are time dependent when viewed by an observer in the NSC frame.

When enforcing *channel boundary conditions* (CBC) on (2-5) we require that all quantities are periodic in the vertical and azimuthal directions, similar to as before, but we require no normal-flow at the channel boundaries. These statements amount to

$$\begin{aligned} f(x, y, z) &= f(x, y + L_y, z), \\ f(x, y, z) &= f(x, y, z + L_z), \\ u &= 0, \quad \text{at } x = 0, L_x, \end{aligned} \quad (10)$$

where, as before, f is any fluid quantity.

2.3. A Pair of Integral Statements

The dynamical equations (2-5) describe the evolution of velocities which are disturbances about a steady rotationally supported flow. As we have stated, the flow appears in these equations in the form of a linear shear. Therefore the steady solution, $\mathbf{u} = 0$, is interpreted as the undisturbed state. We now consider the *total* velocity \mathbf{v} defined as

$$\mathbf{v} \equiv -q\Omega_0 x \hat{\mathbf{y}} + \mathbf{u}. \quad (11)$$

As such the governing equations of motion (2-5) are more concisely written in vector form,

$$\partial_t \mathbf{v} + \mathbf{v} \cdot \nabla \mathbf{v} = -\nabla p + 2\Omega_0 \hat{\mathbf{z}} \times (\mathbf{v} + q\Omega_0 x \hat{\mathbf{y}}), \quad (12)$$

$$\nabla \cdot \mathbf{v} = 0. \quad (13)$$

Note that these equations written in this way have appeared in other works (*e.g.*, Lesur & Longaretti, 2005). Taking the inner product of (12) with \mathbf{v} and following some manipulation yields the following

$$\partial_t \varepsilon + \mathbf{v} \cdot \nabla (\varepsilon + p) = 0, \quad (14)$$

where

$$\varepsilon \equiv \frac{\mathbf{v}^2}{2} - q\Omega_0^2 x^2.$$

With use of the incompressibility condition (13) we may integrate (14) over the full spatial domain to find,

$$\frac{d\mathcal{E}}{dt} = - \int_{\mathcal{S}} (\varepsilon + p) \mathbf{v} \cdot \hat{\mathbf{n}} dS, \quad \mathcal{E} \equiv \int_{\mathcal{V}} \varepsilon dV, \quad (15)$$

in which \mathcal{V} and \mathcal{S} are the volume and surface-boundaries of the domain. The vector $\hat{\mathbf{n}}$ is the unit normal of the bounding surface. The above result is true in general for both linear and nonlinear perturbations. \mathcal{E} is comprised of (a) the term $\mathbf{v}^2/2$ which is the kinetic energy and (b) the potential-like term $-q\Omega_0^2 x^2$. The global integral \mathcal{E} can change due to the influx of ε across the boundaries, *i.e.*, $\int_{\mathcal{S}} \varepsilon \mathbf{v} \cdot \hat{\mathbf{n}} dS$, and through the external work done upon the system denoted by the boundary integral $\int_{\mathcal{S}} p \mathbf{v} \cdot \hat{\mathbf{n}} dS$. The appropriate Bernoulli function for this system is $\varepsilon + p$. The steady values of the function ε and functional \mathcal{E} , ε_0 and \mathcal{E}_0 respectively, are

$$\varepsilon_0 = q \left(\frac{q}{2} - 1 \right) \Omega_0^2 x^2, \quad \mathcal{E}_0 = -\frac{q}{3} \left(1 - \frac{q}{2} \right) \Omega_0^2,$$

where we have assumed here (and throughout) that the azimuthal and vertical periodic scales are $L_z = L_y = 1$ while the radial length scale is $L_x = 1$. The functional \mathcal{E} is analogous to the total energy contained in the flow and its dynamical response (see below) is characterized by the total kinetic energy variations in the box.

By contrast we follow the same procedure as above but consider an energy functional comprised only of the disturbance velocities. In other words one can begin with (3-5) and take its dot product with the disturbance velocity \mathbf{u} . Then, with the use of (2) and either the SBC (8) or the CBC (10), one can integrate over the domain to find

$$\frac{dE}{dt} \equiv \frac{d}{dt} \int_{\mathcal{V}} \xi dV = q\Omega_0 \int_{\mathcal{V}} uv dV; \quad \xi \equiv \frac{1}{2} \mathbf{u}^2. \quad (16)$$

The disturbance energy per unit volume is ξ . The total domain integrated *disturbance energy* is $E \equiv \int_{\mathcal{V}} \xi dV$. The above is known in more general terms as the Reynolds-Orr equation and relates the change of the total disturbance energy to the domain integrated correlation between the radial and azimuthal velocities u and v . This correlation is sometimes referred to as the integrated stress in the flow. In the absence of shear (*i.e.*, $q = 0$), the disturbance energy is conserved.

It is interesting to note the following. Inspection of the Reynolds-Orr relationship says that the domain integrated disturbance energy is not expected to be conserved: so long as there is some correlation between the horizontal and vertical velocities the disturbance energy must fluctuate in time. However from the definitions of \mathcal{E} and E we have

$$\mathcal{E} = E + E_{\text{shear}}; \quad (17)$$

where

$$E_{\text{shear}} \equiv \int_{\mathcal{V}} [-q\Omega_0 x v + \frac{1}{2} q^2 \Omega_0^2 x^2] dV, \quad (18)$$

we see that disturbance energy E is related to \mathcal{E} (the global energy) in an intimate way via E_{shear} , which we consider

to be the disturbance energy affected by the shear in a dynamical sort of way.

To appreciate the significance of these relationships let us see first what happens when CBC are utilized. Applying (10) to (15) shows that

$$\frac{d\mathcal{E}}{dt} = 0, \quad (19)$$

therefore meaning that the fluctuations in E come at the expense of E_{shear} in an equal but opposite way throughout the dynamical response of the flow; *i.e.*, the stresses comprising the RHS of (16) is a measure of the time rate of change between these two forms of measured energy.

(19) also holds for radially (shearwise) localized disturbances in a radially unbounded domain as well. We mean to say that if instead of the CBC (10) we require that the flow be periodic in y and z (again) but that all flow quantities decay sufficiently fast as $x \rightarrow \pm\infty$, then the boundary term in (15) also vanishes and (19) again follows. The same is true if the vertical domain is unbounded instead of periodic - (19) also follows if we then require disturbances to similarly decay as $z \rightarrow \pm\infty$.

By contrast, matters are less clear when shearing boundary conditions are employed. This is because, unlike before, the quantity \mathcal{E} is no longer conserved - it varies with time according to the flux of $\varepsilon + p$ across the boundaries. When the radial boundaries of the periodic box is set at $x = 0$ and $x = 1$ then \mathcal{E} evolves according to

$$\frac{d\mathcal{E}}{dt} = q\Omega_0 \int_{S_1} uvdydz, \quad (20)$$

in which S_1 is the boundary surface at $x = 1$. In general the right-hand side of (20) is not expected to be zero and it means that \mathcal{E} can vary with respect to time when SBC are employed. We note that \mathcal{E} will be conserved for SBC if the disturbances are sufficiently localized in the interior of the computational domain so that there is no power near the bounding surface S_1 (Nusser, 2007).

3. Linear Analysis with SBC

We consider linear perturbations of the equations (2-5). The general linearized equations are,

$$(\partial_t - q\Omega_0 x \partial_y)u - 2\Omega_0 v = -\partial_x P, \quad (21)$$

$$(\partial_t - q\Omega_0 x \partial_y)v + (2 - q)\Omega_0 u = -\partial_y P, \quad (22)$$

$$(\partial_t - q\Omega_0 x \partial_y)w = -\partial_z P, \quad (23)$$

$$\partial_x u + \partial_y v + \partial_z w = 0. \quad (24)$$

We now formally move into the SC frame by introducing the coordinate transformation defined in (7) into (21-24). Also, as a consequence of the coordinate transformation, derivative operations are reexpressed in the SC frame as,

$$\begin{aligned} \partial_x &= \partial_X + q\Omega_0 T \partial_Y, & \partial_y &= \partial_Y, \\ \partial_z &= \partial_Z, & \partial_t &= \partial_T - q\Omega_0 X \partial_Y. \end{aligned} \quad (25)$$

This coordinate transformation is volume preserving since its Jacobian is 1. Since we are considering triply periodic

conditions (in the SC frame) we express all dynamical variables in terms of Fourier modes. Thus if f is some dynamical quantity then we say it is composed of a sum of these waveforms

$$f(X, Y, Z, T) = \sum_{k\alpha\beta} f_{k\alpha\beta}(T) e^{ikX + i\alpha Y + i\beta Z} + c.c. \quad (26)$$

Note that because this is a triple Fourier expansion of inherently real quantities it is enough to restrict all considerations to $0 \leq \beta < \infty$, $-\infty < \alpha < \infty$ and $-\infty < k < \infty$.

Using the above solution ansatz, together with the coordinate transformation (7) and operator reexpression (25), we find that the governing linearized equations for each wavemode (21-24) now appear in the SC frame as,

$$\dot{u}_{k\alpha\beta} - 2\Omega_0 v_{k\alpha\beta} = -i(k + q\Omega_0 T \alpha) P_{k\alpha\beta}, \quad (27)$$

$$\dot{v}_{k\alpha\beta} + (2 - q)\Omega_0 u_{k\alpha\beta} = -i\alpha P_{k\alpha\beta}, \quad (28)$$

$$\dot{w}_{k\alpha\beta} = -i\beta P_{k\alpha\beta}, \quad (29)$$

$$(k + q\Omega_0 T \alpha) u_{k\alpha\beta} + \alpha v_{k\alpha\beta} + \beta w_{k\alpha\beta} = 0, \quad (30)$$

where $\dot{f} \equiv df/dT$. We are left with a set of three first order ODE's plus the incompressibility condition. Taking the divergence of (27-29) and making use of (30) we can express $P_{k\alpha\beta}$ in terms of $u_{k\alpha\beta}$ and $v_{k\alpha\beta}$, that is

$$P_{k\alpha\beta} = 2\Omega_0 i \frac{(1 - q)\alpha u_{k\alpha\beta} - (k + q\Omega_0 T \alpha)v_{k\alpha\beta}}{(k + q\Omega_0 T \alpha)^2 + \alpha^2 + \beta^2}. \quad (31)$$

Using a fourth order Runge-Kutta scheme we evolve (27-29) in time using (30) to set the initial conditions and (31) to calculate the pressure at each time step (see below).

Note that Balbus & Hawley (2006) explicitly demonstrate that the single waveform (26) is an exact solution of the nonlinear equations of this system, *i.e.*, (21-24) with the nonlinear advection terms included. Had we retained those terms and applied a single waveform from the general ansatz (26) then one recovers exactly (27-30).

Before jumping head-on into numerical results of these linear equations it is both instructive and useful to also determine asymptotically valid solutions. We do this both to gain a sense of what to expect mathematically and to verify that the numerical scheme (here the fourth order Runge-Kutta) is indeed capturing the dynamical behavior. This is accomplished by further combining the equations into a single one for the evolution of $u_{k\alpha\beta}$. In particular we take the derivative of (27) with respect to time and then reexpress the result using (28) and (31). This procedure yields a single second order ODE for $u_{k\alpha\beta}$ ⁴,

$$\begin{aligned} \ddot{u}_{k\alpha\beta} + \frac{4q\Omega_0\alpha(k + q\Omega_0 T \alpha)}{(k + q\Omega_0 T \alpha)^2 + \alpha^2 + \beta^2} \dot{u}_{k\alpha\beta} + \\ \frac{2(q\Omega_0\alpha)^2 + 2(2 - q)\Omega_0^2\beta^2}{(k + q\Omega_0 T \alpha)^2 + \alpha^2 + \beta^2} u_{k\alpha\beta} = 0. \end{aligned} \quad (32)$$

⁴ Solutions to this equation may actually be analytically expressed in terms of hypergeometric functions (Abramowitz & Stegun, 1972, Johnson and Gammie, 2005). However, the type of hypergeometric these turn out to be cannot be expressed in terms of simpler functions. This is why we pursue numerical solutions together with accompanying asymptotic expressions.

For long enough times, namely much longer than $\frac{2k}{3\alpha}$ or $\frac{2}{3}[1 + (\frac{\beta}{\alpha})^2]^{\frac{1}{2}}$ (32) assumes the form of an Euler-Cauchy equation,

$$T^2 \ddot{u}_{k\alpha\beta} + 4T \dot{u}_{k\alpha\beta} + 2 \left[1 + \frac{2-q}{q^2} \left(\frac{\beta}{\alpha} \right)^2 \right] u_{k\alpha\beta} = 0, \quad (33)$$

which has exact solutions depending on the value of

$$\Sigma \equiv \frac{4\omega_\varepsilon^2}{\Omega_0^2 q^2} \left(\frac{\beta}{\alpha} \right)^2, \quad \omega_\varepsilon^2 \equiv \Omega_0^2 2(2-q), \quad (34)$$

where ω_ε is the *epicyclic frequency*. The quality of the solutions depends on whether Σ is larger, equal to or smaller than 1, or in other words whether the ratio $|\frac{\alpha}{\beta}|$ is larger, equal to or smaller than $\frac{4}{3}$ for $q = 3/2$. We define a new parameter, Π_\pm as,

$$\Pi_\pm = \pm \frac{\sqrt{1-\Sigma}}{2} \quad (35)$$

The long time behavior of $u_{k\alpha\beta}$, $v_{k\alpha\beta}$ and $w_{k\alpha\beta}$ for Keplerian flow ($q = 3/2$) is,

$$\lim_{t \rightarrow \infty} u_{k\alpha\beta} = T^{\Pi_\pm - \frac{3}{2}}, \quad \lim_{t \rightarrow \infty} v_{k\alpha\beta}, w_{k\alpha\beta} \propto T^{\Pi_\pm - \frac{1}{2}} \quad (36)$$

The three cases are itemized below:

(i) for $\Sigma < 1$, that is $|\frac{\alpha}{\beta}| > \frac{4}{3}$, the long time behavior is,

$$\begin{aligned} \lim_{T \rightarrow \infty} u_{k\alpha\beta} &= \left(A_1 T^{\frac{\sqrt{1-\Sigma}}{2}} + A_2 T^{-\frac{\sqrt{1-\Sigma}}{2}} \right) \cdot T^{-\frac{3}{2}} \\ \lim_{T \rightarrow \infty} v_{k\alpha\beta}, w_{k\alpha\beta} &= \left(B_1 T^{\frac{\sqrt{1-\Sigma}}{2}} + B_2 T^{-\frac{\sqrt{1-\Sigma}}{2}} \right) \cdot T(37) \end{aligned}$$

(ii) for $\Sigma = 1$, that is $|\frac{\alpha}{\beta}| = \frac{4}{3}$, the long time behavior is,

$$\begin{aligned} \lim_{T \rightarrow \infty} u_{k\alpha\beta} &= (A_1 + A_2 \ln T) \cdot T^{-\frac{3}{2}} \\ \lim_{T \rightarrow \infty} v_{k\alpha\beta}, w_{k\alpha\beta} &= (B_1 + B_2 \ln T) \cdot T^{-\frac{1}{2}} \end{aligned} \quad (38)$$

(iii) for $\Sigma > 1$, that is $|\frac{\alpha}{\beta}| < \frac{4}{3}$,

$$\begin{aligned} \lim_{T \rightarrow \infty} u_{k\alpha\beta} &= \left[A_1 \cos \left(\frac{1}{2} \sqrt{|\Sigma| - 1} \ln T \right) + \right. \\ &\quad \left. A_2 \sin \left(\frac{1}{2} \sqrt{|\Sigma| - 1} \ln T \right) \right] \cdot T^{-\frac{3}{2}} \\ \lim_{T \rightarrow \infty} v_{k\alpha\beta}, w_{k\alpha\beta} &= \left[B_1 \cos \left(\frac{1}{2} \sqrt{|\Sigma| - 1} \ln T \right) + \right. \\ &\quad \left. B_2 \sin \left(\frac{1}{2} \sqrt{|\Sigma| - 1} \ln T \right) \right] \cdot T^{-\frac{1}{2}} \end{aligned} \quad (39)$$

It is apparent from this asymptotic form that all solutions are stable, showing algebraic decay as $T \rightarrow \infty$.

3.1. Results

Using a fourth order Runge-Kutta scheme we evolve equations (27)-(29), using (31) to determine the value of $P_{k\alpha\beta}$ for each time step, which was taken to be 0.01 (1 box

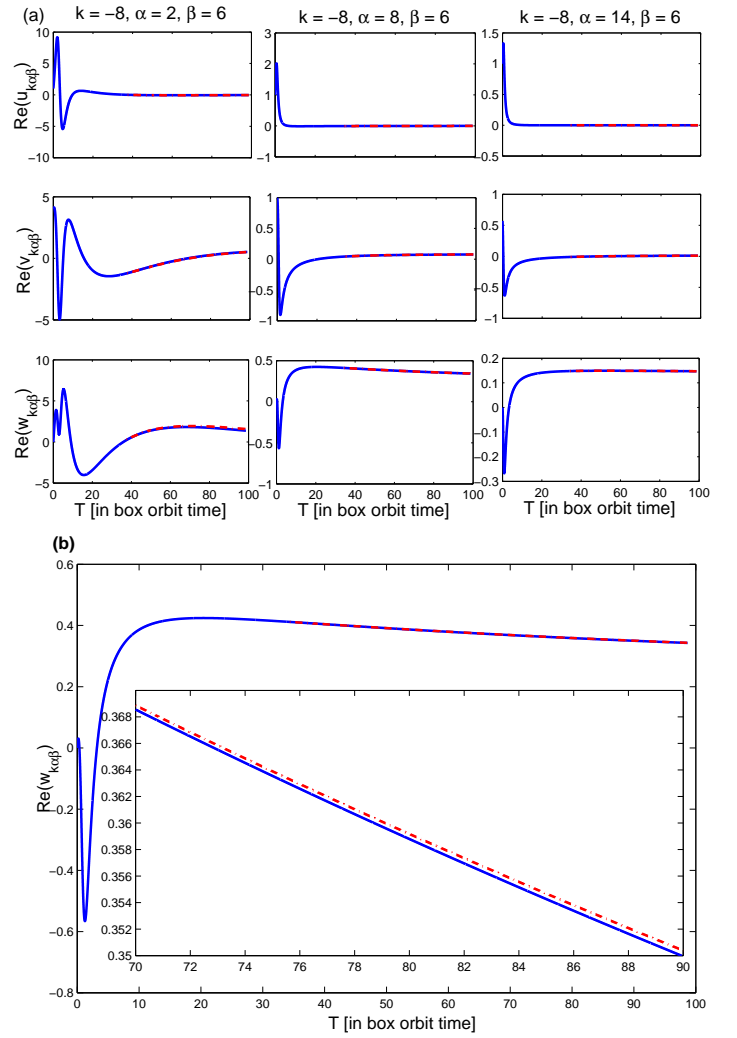


Fig. 1. (a) The numerical solution (solid blue lines) for three different cases of k , α and β , in comparison with the asymptotic solution (dashed red lines). (left) $k = -8$, $\alpha = 2$ and $\beta = 6$; (center) $k = -8$, $\alpha = 8$ and $\beta = 6$; (right) $k = -8$, $\alpha = 14$ and $\beta = 6$. T is given in box orbit time. (b) A magnification of one of the plots showing the agreement between the two solutions.

orbit time = 2π). For a long enough time, T_0 , the coefficients of the asymptotic solution in question, *i.e.*, either of (37-39), are determined using the values of the numerical solutions at that time, *e.g.*, $u_{k\alpha\beta}(T_0)$, $\dot{u}_{k\alpha\beta}(T_0)$ (and the same as well for $v_{k\alpha\beta}$ and $w_{k\alpha\beta}$). Figure 1(a) displays three solutions, numerical solutions in solid blue lines and asymptotic solutions in dashed red lines (in all figures T is given in box orbit time). These are just three examples representing the three distinct cases of $\Sigma > 1$, $\Sigma = 1$ and $\Sigma < 1$. As shown in this figure, the numerical solution of the code is in very good agreement with the asymptotic solution (usually around 1-5% deviation between the two solutions). Figure 1(b) shows a magnification of a region of the solution for $v_{k\alpha\beta}$ that shows the good compatibility between the asymptotic and numerical solutions.

According to the asymptotic forms we have derived, all linear perturbations decay algebraically at long times. Nonetheless, we find that for all perturbations with $\frac{k}{\alpha} < 0$ there is a window of growth in the disturbance E energy before final decay. The extent of growth and its duration in time is a function of the magnitude of $|\frac{k}{\alpha}|$ which, in other words, is a measure of the perturbation's stream-wise streakiness. As we was noted in the introduction, the streaky perturbation *must be leading*, (*i.e.*, $\frac{k}{\alpha} < 0$) in order for there to manifest growth. With pronounced streakiness, the growth is both stronger and lasts for a longer period in time. Figure (2) summarizes this point in showing the great effect $|\frac{k}{\alpha}|$ has on the transient growth for four values of the streakiness.

Moreover, as seen in Figure (3), the ratio $\frac{\alpha}{\beta}$ determines the qualitative behavior of the temporal response. In short, after the first peak is achieved, whether or not $\frac{\alpha}{\beta}$ is greater or less than $4/3$ (for $q = 3/2$) determines whether there is zero, one or infinite secondary peaks in the response. We know from the asymptotic forms that for $|\frac{\alpha}{\beta}| < 4/3$ the velocity profiles show decaying oscillations with a time dependent frequency as evident by the $\ln(T)$ dependence in the argument of (39). This oscillation tendency carries over into the disturbance energy as well. When $|\frac{\alpha}{\beta}| \geq 4/3$, there are no oscillations expected for asymptotic times.

The numerical solutions add to this picture by revealing what happens at the short times. The general feature is that there is usually one very strong peak that occurs for leading waves, irrespective of the value of $|\frac{\alpha}{\beta}|$. Only for long times does one observe the behavior predicted from the asymptotic theory in particular:

- (i) For $|\frac{\alpha}{\beta}| < \frac{4}{3}$ the disturbance energy has an infinitude of peaks with the first of these being pronounced and distinct. Soon after this initial spike, the perturbation energy quickly decays to the order of magnitude of the initial energy it began with, *i.e.*, E_0 . Judging from the asymptotic solutions, under these conditions these quantities ought to show successive peaks but the period of "return" for them goes like $\ln(T)$. As such we observe, at most, only two such peaks as it was not practical to run the simulations long enough to see subsequent ones. Its overall envelope continues its eventual decay to zero as $T \rightarrow \infty$.
- (ii) In the case of $|\frac{\alpha}{\beta}| = \frac{4}{3}$ and $|\frac{\alpha}{\beta}| > \frac{4}{3}$, the second spike's peak is lower but the decay is longer than that of the first case, and the energy remains larger than E_0 in an order of magnitude, or even larger, for a long time (in this case for instance, after almost 10 box orbit times $\frac{E_{k\alpha\beta}}{E_0} \approx 12$ and after almost 50 box orbit times $\frac{E_{k\alpha\beta}}{E_0} \approx 4.5$). Of course, as the asymptotic theory shows, even this energy must also decay at asymptotically large times.

- (iii) In the $|\frac{\alpha}{\beta}| > \frac{4}{3}$ case the second peak is almost flat and decays even slower than in the $|\frac{\alpha}{\beta}| = \frac{4}{3}$ case (in this case for instance, after almost 10 box orbit times $\frac{E_{k\alpha\beta}}{E_0} \approx 6.7$ and after almost 150 box orbit times $\frac{E_{k\alpha\beta}}{E_0} \approx 3.6$).

In Figure (4) it is shown that the ratio $\frac{k}{\beta}$ effects the behavior (the value, not the shape of the graph) of $P_{k\alpha\beta}$, and $w_{k\alpha\beta}$, but does not effect $u_{k\alpha\beta}$ and $v_{k\alpha\beta}$. Moreover the ratio does not effect the peak in the energy, $E_{k\alpha\beta}$, and only effects the value of the energy after the peak (because of the effect on $w_{k\alpha\beta}$ which is the main contributor to the energy after the peak).

4. Linear Analysis with CBC

In considering the response of the flow in the channel model we shall assume initially the general form

$$f(x, y, z, t) = f_{\alpha\beta}(x, t)e^{i\alpha y + i\beta z} + c.c. \quad (40)$$

With this form the linearized equations of motion now read,

$$(\partial_t - iq\Omega_0 x\alpha)u_{\alpha\beta} - 2\Omega_0 v_{\alpha\beta} = -\partial_x P_{\alpha\beta}, \quad (41)$$

$$(\partial_t - iq\Omega_0 x\alpha)v_{\alpha\beta} + (2 - q)\Omega_0 u_{\alpha\beta} = -i\alpha P_{\alpha\beta}, \quad (42)$$

$$(\partial_t - iq\Omega_0 x\alpha)w_{\alpha\beta} = -i\beta P_{\alpha\beta}, \quad (43)$$

$$\partial_x u_{\alpha\beta} + i\alpha v_{\alpha\beta} + i\beta w_{\alpha\beta} = 0. \quad (44)$$

The boundary condition are that $u_{\alpha\beta} = 0$ at $x = 0, 1$. These equations may be reduced to a single one for $u_{\alpha\beta}$,

$$(\partial_t - iq\Omega_0 x\alpha)^2 (\partial_x^2 - \beta^2 - \alpha^2)u_{\alpha\beta} = \omega_c^2 \beta^2 u_{\alpha\beta}. \quad (45)$$

A full breadth of normal-mode solutions of the form $\exp(i\omega t)$ exist only for certain combinations of β and α . To see what the restriction is in the following we perform a normal analysis and determine precisely under what conditions this circumstance occurs. Thus, assuming the normal mode form

$$u_{\alpha\beta} = \hat{u}_{\alpha\beta} e^{i\omega t},$$

into the governing equations (41)-(44) and manipulating the result into a single equation for $\hat{u}_{\alpha\beta}$ results in

$$(\omega - q\Omega_0 x\alpha)^2 (\partial_x^2 - \beta^2 - \alpha^2)\hat{u}_{\alpha\beta} + \omega_c^2 \beta^2 \hat{u}_{\alpha\beta} = 0. \quad (46)$$

4.1. $\alpha = 0$

As a point of departure and to gain a little insight into the general behavior of these disturbances we consider the limit where $\alpha = 0$ in (46). Applying the boundary conditions on u yields the dispersion relationship

$$\omega^2 = \frac{\omega_c^2 \beta^2}{n^2 \pi^2 + \beta^2}; \quad n = 1, 2, 3 \dots \pm \infty \quad (47)$$

with the eigenfunction solutions,

$$\hat{u}_{\beta} = A_{\beta} \sin(n\pi x). \quad (48)$$

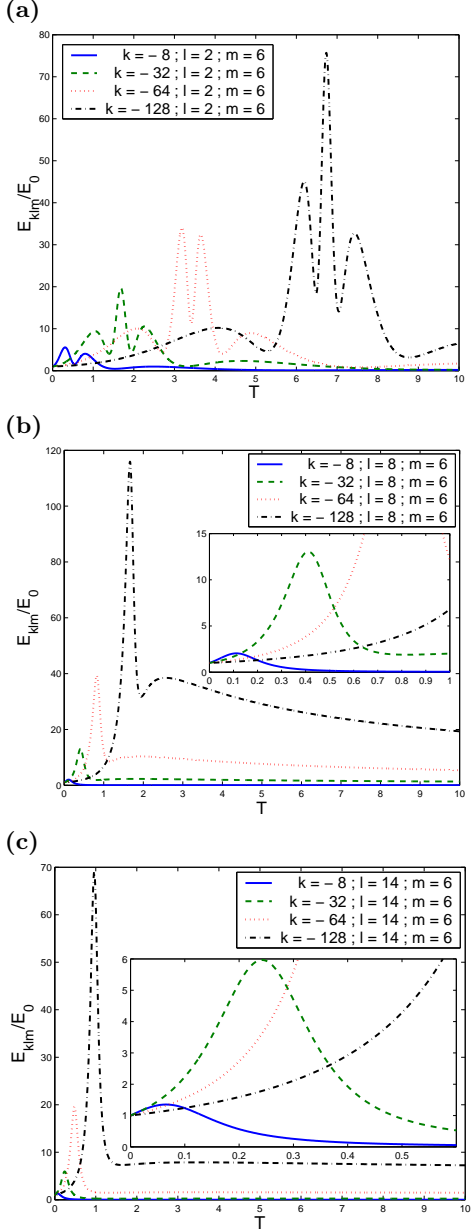


Fig. 2. Four cases differed by the ratio $\frac{k}{l}$ showing the great effect this ratio has on the transient growth the modes undergo.

in which A_β is an arbitrary amplitude. In other words, for given values of β there are a countably infinite number of quantization values labeled by n . Furthermore, in the limit when $\beta \rightarrow \infty$ the oscillations cluster near the points $\pm\omega_e$. These modes look like classic inertial oscillations with frequencies clustering near $\pm\omega_e$ as $\beta \rightarrow \pm\infty$ respectively.

4.2. $\alpha \neq 0$.

The solution to (46) subject to the boundary conditions that $\hat{u}_{\alpha\beta} = 0$ at $x = 0, 1$ is given by

$$\hat{u}_{\alpha\beta} = A(\omega - q\Omega_0 x\alpha)^{1/2} \left\{ J_\nu [i\lambda(\omega - q\Omega_0 x\alpha)] Y_\nu [i\lambda\omega] - \right.$$

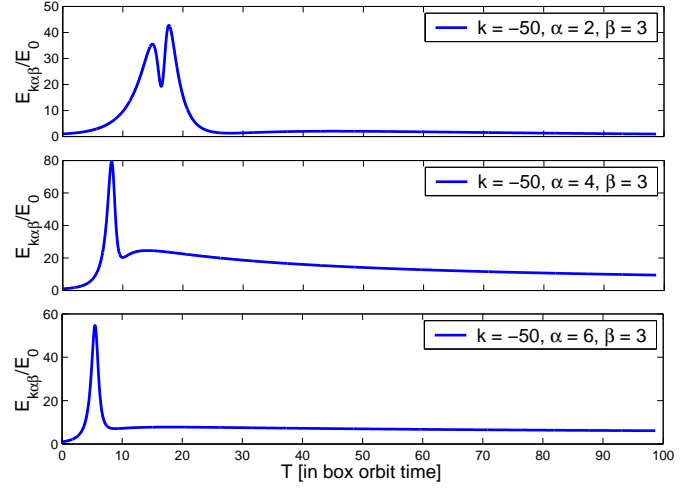


Fig. 3. The normalized energy for the three different cases of $\frac{\alpha}{\beta}$, where $k = -50$, $\beta = 3$ and $\alpha = 2, 4, 6$, showing the effect $\frac{\alpha}{\beta}$ has on peaks in the energy.

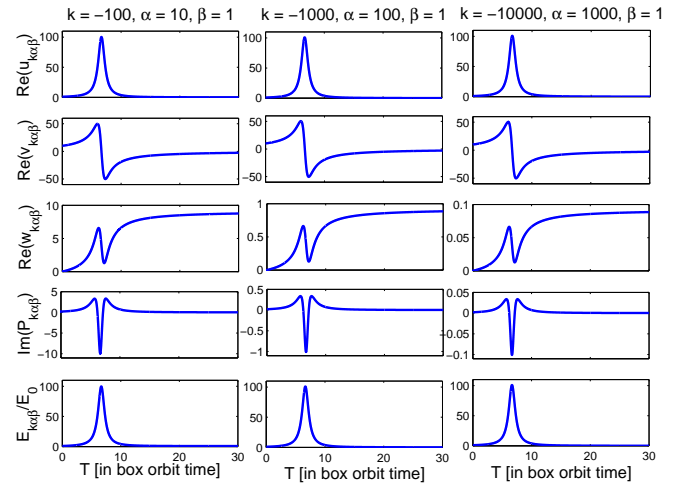


Fig. 4. Three cases, all with $\Sigma < 1$, and a fixed ratio between k and α , showing that the ratio between k and β has no significant effect on the solution.

$$Y_\nu [i\lambda(\omega - q\Omega_0 x\alpha)] J_\nu [i\lambda\omega] \Big\}, \quad (49)$$

where

$$\lambda^2 = \frac{\beta^2 + \alpha^2}{q^2 \Omega_0^2 \alpha^2}, \quad \nu^2 = \frac{1 - \Sigma}{4}, \quad (50)$$

where J_ν and Y_ν are Bessel Functions of order ν , and where Σ is as defined in (34). The quantization condition on ω is

$$(\omega - \omega_\infty)^{1/2} \left\{ J_\nu [i\lambda(\omega - \omega_\infty)] Y_\nu [i\lambda\omega] - Y_\nu [i\lambda(\omega - \omega_\infty)] J_\nu [i\lambda\omega] \right\} = 0. \quad (51)$$

The governing equation and its solution has a regular singular point for $\omega = \omega_\infty \equiv q\Omega_0\alpha$ at the point $x = 1$. As

it turns out, the solution automatically satisfies its requisite boundary condition at $x = 1$ when $\omega = \omega_\infty$. These modes are the fundamental structures that constitute the so-called *wallmodes* that give rise to the stratorotational instability in systems supporting a vertical gravitational field (Yavneh *et al.*, 2001, Dubrulle *et al.*, 2005 Umurhan, 2006).

We observe that if ν , as appearing, is a real quantity then there is no way for the quantization condition to be met by real values of ω (other than the single value ω_∞) according to the known behavior of the Bessel functions (Abramovitch & Stegun, 1972). This means that if $\Sigma < 1$, then *there is only one normal mode solution for this problem.*

For $\Sigma > 1$ there exists a countably infinite set of normal-mode solutions (overtones) as per the theory of Bessel functions (see again Abramovitch & Stegun, 1972). This behavior contains the $\alpha = 0$ theory since the latter is formally the limit where Σ tends to infinity.

Nevertheless, inferring the dynamical content of the disturbances, including the shape of the eigenfunctions and the general formulae for the dispersion relationship, is not easy. One can more transparently study the behavior of these features if an asymptotic solution for $u_{\alpha\beta}$ is developed instead. This can be done for the small limiting values of β and α . The result contains information regarding the character change of the solutions alluded to above.

In particular, given ϵ to be a small parameter and that

$$\beta = \epsilon\beta_1, \quad \alpha = \epsilon\alpha_1,$$

then by adopting the following expansions

$$\omega = \epsilon\omega_1 + \epsilon^3\omega_3 + \dots, \quad \hat{u}_{\alpha\beta} = u_0 + \epsilon^2u_2 + \dots,$$

we find that the lowest order solutions depend critically on the parameter Σ_1 defined by,

$$\Sigma_1 = \frac{4\omega_e^2\beta_1^2}{q^2\Omega_0^2\alpha_1^2}.$$

Evidently, Σ_1 is really a reexpression of Σ . In particular, the linear equation (46) in this limit becomes to lowest order

$$\left[\frac{\partial^2}{\partial x^2} + \frac{\omega_e^2\beta_1^2}{(\omega_1 - q\Omega_0x\alpha_1)^2} \right] u_0 = 0. \quad (52)$$

The solutions for u_0 are

$$u_0 = A_0 \left(1 - \frac{q\Omega_0x\alpha_1}{\omega_1} \right)^{1/2+\delta} - A_0 \left(1 - \frac{q\Omega_0x\alpha_1}{\omega_1} \right)^{1/2-\delta}, \quad (53)$$

$$\delta = \sqrt{\frac{1 - \Sigma_1}{4}},$$

where A_0 is an arbitrary amplitude. By construction the solution (53) satisfies the condition $u_0(0) = 0$. Given this asymptotic form, it becomes clear now how the general solution also predicts the absence of normal-mode solutions if $\Sigma_1 < 1$

First we focus on solutions for when $\Sigma_1 > 1$. The lowest order velocity is,

$$u_0 = A_0 \left(1 - \frac{q\Omega_0x\alpha_1}{\omega_1} \right)^{1/2} \sin \left[|\delta| \ln \left(1 - \frac{q\Omega_0x\alpha_1}{\omega_1} \right) \right], \quad (54)$$

where A_0 is in general an arbitrary amplitude - however, in order to compare these solutions to the exact ones we shall choose $A_0 = 1/2\delta$ implying that $\frac{du_0}{dx}|_{x=0} = 1$. The quantization condition on ω_1 , resulting from imposing the constraint that $u_0(1) = 0$, amounts to

$$\omega_1 = \frac{q\Omega_0\alpha_1}{1 - e^{|\delta|}}, \quad n = \pm 1, \pm 2, \dots \quad (55)$$

The index n is a label designating the particular overtone in question. There are an infinite number of radial overtones for any allowable pair of β_1 's and α_1 's.

When $\Sigma_1 < 1$ then the solution satisfying the boundary condition at $x = 0$ is

$$u_0 \sim \left(1 - \frac{q\Omega_0x\alpha_1}{\omega_1} \right)^{1/2+\delta} - \left(1 - \frac{q\Omega_0x\alpha_1}{\omega_1} \right)^{1/2-\delta}. \quad (56)$$

Since under these conditions $0 < \delta < 1/2$, the solution for u_0 has a regular singular point at $x = \omega_1/q\Omega_0\alpha_1$. Unlike when $\Sigma_1 > 1$, there is only one eigenmode of the system corresponding to the eigenvalue $\omega_1 = q\Omega_0\alpha_1$, as was alluded to before. In this circumstance the frequency spectrum is continuous (Case, 1960).

In a more general sense: when $\Sigma < 1$, aside from the mode $\omega = \omega_\infty$, the response of the flow must be considered as an initial value problem since the system supports no normal modes. When $\Sigma > 1$ then there are two branches of normal modes (*i.e.*, overtones) clustering about $\omega = 0$ and $\omega = \omega_\infty$ - in general the frequencies around which the overtones cluster correspond to wavespeeds (*i.e.*, $c = \omega/\alpha$) that equal the flow speeds at the two channel boundaries.

We show in Figure (5) a comparison of the eigenfunctions and eigenfrequencies between the asymptotic solutions derived and the exact solutions in the event where $\Sigma > 1$. We depict the results only for overtones with $n \geq 1$. The reason is that (46) remains unchanged after applying the spatial reflection operation about the point $x = 1/2$ together with the frequency reflection/shift $\omega \rightarrow -\omega + q\Omega_0\alpha$. In other words this means to say that a given eigensolution $\hat{u}_{\alpha\beta}^{(+)}(x)$ with eigenfrequency ω_+ generates another eigensolution $\hat{u}_{\alpha\beta}^{(-)}$ with eigenfrequency $\omega_- = -\omega_+ + q\Omega_0\alpha$ such that $\hat{u}_{\alpha\beta}^{(-)}$ is the mirror reflection of $\hat{u}_{\alpha\beta}^{(+)}$ about $x = 1/2$. It is in this way overtones with positive n relate to their counterparts with negative values of n . In general we see that the approximate theory - including the predicted eigenfrequencies - are good even for order 1 values of α and β , but the theory begins to breakdown when they exceed order 1 values.

5. Summary and Discussion

We shall recap the major findings of this work and offer some comments and reflections about their possible impact on the questions posed in the Introduction.

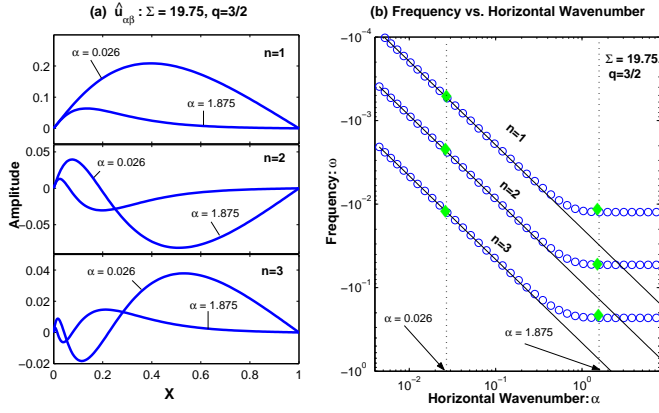


Fig. 5. Results from normal mode theory in which $\Sigma = 19.75$ and $q = 3/2$. (a) The exact eigenfunctions for $\hat{u}_{\alpha\beta}$ depicted for the first three overtones each at two values of α . The eigenfunctions developed via the asymptotic theory lie exactly on the eigenfunctions for $\alpha = 0.02$. (b) The frequencies ω as a function of α for the first three overtones are shown (open circles). The predicted frequencies using the asymptotic theory are shown with solid lines. The values corresponding to the eigenfunctions depicted in the left panel are designated with diamonds. Note that only the positive overtones (*i.e.*, $n > 0$) are shown here - the negative overtones are reflection symmetric about $x = 1/2$ as discussed in the text.

- The analysis of linearized disturbances subject to channel boundary conditions shows that Σ determines the quality of the response. For given azimuthal and vertical wavenumbers (α and β): the system admits a countably infinite number of normal mode solutions (inertial oscillations) for $\Sigma > 1$, which includes a wallmode-type eigenmode (Yavneh et al, 2001), while on the other hand, when $\Sigma < 1$ then the system admits only the single wallmode-type eigenmode which means that disturbances under these conditions in general require an initial value problem treatment (which we have not done here).

With respect to the question of dynamics of wall-bounded rpC, these results are quite suggestive. Rincon *et al.* (2006) showed that Rayleigh-stable anticyclonic rpC flow appears not to show a transition into a turbulent state in the manner in which transition is observed in pC flow (*e.g.*, Waleffe, 2003). The strategy in those problems is to identify *steady* nonlinear solutions of the flow (usually by some continuation method from known solutions in otherwise unstable parameter regimes, *e.g.*, Nagata, 1990, or forcing methods, Waleffe, 2003) and study their stability properties. If there are a collection of steady nonlinear structures, some of which unstable, then the transition into a turbulent state is thought to be approached. These states get easily triggered (bypass mechanism) because small scale disturbances in pC flow get amplified due to the lift-up effect. Rincon *et al.* (2006) however show that there are two problems with this approach when employed

to identify structures of rpC flow near the Rayleigh-stable line (*e.g.*, near $q = 2$ for $\text{Re} \rightarrow \infty$): that steady structures could not be identified and that the anti lift-up effect induces azimuthal velocity fields which are quite small (in proportion to $1/\text{Re}$) in comparison to the azimuthal velocity fields generated by the lift-up effect in pC flow.

Since the linear analysis of the inviscid Rayleigh-stable rpC shows that for a given α and β there are conditions where there exists a countable number of oscillating modes, perhaps one might need to consider identifying oscillating nonlinear structures instead of steady ones. Perhaps one strategy would be to (i) identify oscillating nonlinear states in the infinite Reynolds Number case ($\text{Re} = \infty$) and then (ii) ratchet down Re and follow/study the structures and their activity until either (iii) one identifies a Re of transition, if a unique one exists free of hysteretic effects or determine if, as Rincon *et al.* (2006) suggest, rpC flow exhibits the character of a chaotic saddle⁵ which is heavily dependent on initial conditions (see also Faisst & Eckhardt, 2004).

- The linear theory analysis of disturbances subject to SBC reveal a number of things which we itemize here. (i) The ratio $|k/\alpha|$ is probably the most significant quantity measuring the maximal amplification of a given disturbance, where k is the radial wavenumber. The time in which the maximal amplification is achieved, as well as the overall relative amplitude the disturbance achieves, is directly proportional to this measure of the streamwise streakiness of the perturbation. (ii) The ratio $|k/\beta|$ has no significant effect on the evolution of the linear dynamics of the problem. (iii) The ratio $|\alpha/\beta|$ determines the shape of the peaks in the flow variables including the disturbance energies. (iv) The value of the parameter Σ effects the quality of the long-time behavior of all solutions. If $\Sigma > 1$ then the modes show monotonic decay while if $\Sigma < 1$ then there are oscillations (with a time dependent period $\sim \ln(T)$) in the decaying response.

In comparison to CBC, dynamics subject to SBC probably lead to entirely different phenomena given the algebraic response and eventual decay of individual waves. Balbus & Hawley (2006) have observed that the individual wavemodes are also exact solutions to the full (non-linear) equations of motion. As such these modes have no self-interaction energy - the only way to distribute their energy is through mode-mode interactions which results in power generated at smaller scales which is presumably lost. However it is those wave-modes with power at very small scales (*i.e.*, leading wave-modes with streaky structure) that can rise in amplitude after some time. In or-

⁵ An example of a chaotic saddle would be the dynamics inside a box with a small hole somewhere on the boundary (imagine a pinball machine) - the dynamics may appear to be chaotic but is fundamentally transient as the particle eventually escapes through the hole (Faisst & Eckhardt, 2004). The time for escape will sensitively depend on the initial conditions.

der to further explore this type of action one must somehow, either by numerical or analytic means, understand better the time-scales associated with the wave-wave cascade of power onto small-scale modes and compare this with the amplification time-scales associated with those modes. It is likely that a proper (numerical) evaluation of this process critically requires sufficient resolution (especially radial resolution) to allow power into those modes (*e.g.*, Longaretti, 2002, Jimenez et al, 2006). High resolution simulations may indicate that such flows may be exhibiting the characteristics of a chaotic saddle too.

- We demonstrated that \mathcal{E} is conserved for (but not limited to) inviscid rpC flow that is (i) subject to CBC or (ii) disturbances which are streamwise (azimuthally) and spanwise (vertically) periodic, shearwise (radially) localized, on a radially unbounded domain or, (iii) streamwise periodic, spanwise and shearwise localized disturbances on radial/vertical domains that are unbounded. The important characteristic of all these circumstances is that disturbances are localized and that the total energy \mathcal{E} of the system is conserved, which includes the total kinetic energy and not just the energy in the disturbances. By contrast, \mathcal{E} is not conserved in disturbances subject to SBC but evolves according to the following generalization of (20)

$$\frac{d\mathcal{E}}{dt} = q\Omega_0 \oint_{\mathcal{S}} xuvd\hat{\mathbf{s}},$$

where $\hat{\mathbf{s}}$ is the surface element of the bounding surface, \mathcal{S} , of the (sheared) periodic box.

For an individual wavemode solution satisfying SBC, *i.e.*, one wavemode of (26) with given k, α and β , it follows that

$$\frac{d\mathcal{E}}{dt} = \frac{dE}{dt},$$

where E is the disturbance kinetic energy of the wavemode (see 16). From (17) it follows that these disturbances conserve the shear energy E_{shear} as defined in (18). It remains to be understood what are the consequences and physical meaning to the conservation of E_{shear} .

These observations underscore the need for further analysis. It is apparent that the dynamics of rpC flows with confined/localized disturbances must be different than those of flows subject to shearing boundary conditions simply because of the different consequences that must follow on account of the conservation properties of \mathcal{E} . The linear theory discussed in this work suggests that these differences somehow manifest themselves in the temporal fate of disturbances, *e.g.*, flows with channel boundary conditions can support modes that neither grow nor decay while modes subject to shearing boundary conditions show decay. It seems worthwhile to further understand what these differences are and what they may mean in order to help interpret the results coming from such studies (also see Dubrulle, *et al.*, 2004).

6. Acknowledgements

The authors would like to thank the Israeli Science Foundation for making this work possible. We also express our gratitude to Adi Nusser, Giora Shaviv and Edward A. Spiegel for the valuable insights they shared with us. This work was partially supported by BSF grant number 0603414082.

References

- Abramowitz, M. & Stegun, I. A., 1972, Handbook of Mathematical Functions, Dover, New York
- Afshordi, N., Mukhopadhyay, B., & Narayan, R., 2005, ApJ, 629, 373
- Balbus, S.A. & Hawley, J.F., 2006, ApJ, 652, 1020
- Balbus, S.A., Hawley, J.F., 1992, ApJ, 400, 610
- Butler, K.M. & Farrell, B.F., 1992, Phys. Fluids A, 4, 1637
- Case, K.M., 1960, Phys. of Fluids, 3, 143
- Chagelishvili, G.D., Zahn, J.-P., Tevzadze, A. G., & Lominadze, J.G., 2003, A&A, 402, 401
- Drazin, P.G. & Reid, W.H., 1981, Hydrodynamic Stability, Cambridge.
- Dubrulle B., Marie L. , Normand Ch., Richard D. , Hersant F. & Zahn J.-P. 2004, A&A, 429, 1
- Faisst, H. & Eckhardt, B., 2004, J. Fluid Mech., 504, 343
- Frank, J., King, A.R., Raine, D.J., 2002, Accretion Power in Astrophysics, 3-rd ed., Cambridge.
- Goldreich, P. & Lynden-Bell, D., 1965, MNRAS, 130, 125
- Hawley, J.F., Balbus, S.A., & Winters, W., 1999, ApJ, 518, 394
- Ioannaou, P.J. & Kakouris, A., 2001, ApJ, 550, 931
- Ji. H., Burin, M., Schartman, E. & Goodman, J., 2006, Nature, 444, 343
- Jiménez, J., Kassinos, S.C. & Wray, A.A., 2006, Proceedings of the Summer Program 2006 (NASA Ames Research Center), 5
- Johnson, B.M. & Gammie, C.F., 2005, ApJ, 626, 978
- Lesur, G. & Longaretti, P.-Y., 2005, 444, 25
- Longaretti, P.-Y., 2002, ApJ, 587
- Lynden-Bell, D. & Pringle, J.E., 1974, MNRAS, 168, 603
- Mukhopadhyay, B., Afshordi, N., & Narayan, R., 2005, ApJ, 629, 383
- Nagata, M., 1986, JFM, 169, 229
- Nusser, A., 2007, private communication.
- Rincon, F., Ogilvie, G. I. & Cossu, C., 2007, A&A, 463 817
- Rogallo, R., 1981, Numerical Experiments in Homogeneous Turbulence (Technical Memo 81315, Moffett Field, NASA/Ames)
- Schmid, P. J. & Henningson, D.S., 2001, Stability and Transition in Shear Flows, Springer
- Sternberg, A., 2005, A search for Hydrodynamical Instabilities in Accretion Disks (Masters Research Thesis, The Technion).
- Umurhan, O.M. & Regev, O., 2004, A&A, 427, 855
- Waleffe, F., 1995, Phys. Fluids, 7, 3060
- Waleffe, F., 1997, Phys. Fluids, 9, 883
- Waleffe, F., 2003, Phys. Fluids, 15, 1517
- Williams, P.T., 2000, Topics in Astrophysical Turbulence (Ph.D. Dissertation, University of Texas)
- Williams, P.T., 2006, astro-ph/0607282
- Yavneh, I., McWilliams J.C. & Molemaker, M.J. 2001, J. Fluid Mech., 448, 1
- Yecko, P.A. 2004, A&A, 425, 385-393